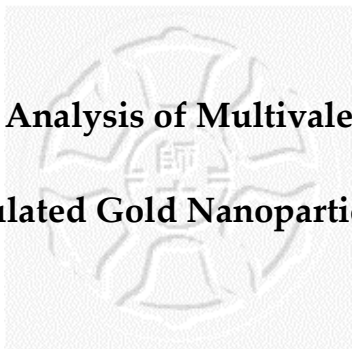


Chapter 4.

Quantitative Analysis of Multivalent Interactions of Carbohydrate-Encapsulated Gold Nanoparticles with Concanavalin A



4.1. Introduction

Multivalent interactions between cell surface receptors and carbohydrates have been discovered in a number of biological processes including fertilization, proliferation, viral/bacterial infection and the inflammatory response.¹ Because of the simultaneous binding of multiple ligands on one biological entity to multiple receptors on another, the multivalent interactions are often with high binding affinity and specificity. A number of diverse scaffolds have been generated for multivalent carbohydrate ligand presentation.² Low-molecular weight displays,³ copolymers,⁴ dendrimers,⁵ nanoparticles,⁶ and liposomes,⁷ for examples, have been employed as powerful carriers to present carbohydrate ligands in polydisperse, linear or globular architectures. In particular, LewisX (LeX, a trisaccharide antigen) encapsulated on gold nanoparticles,⁶ mimicking glycosphingolipid clusters, exhibited significantly enhanced affinity and selectivity as compared with LeX monomers. However, the multivalent binding between carbohydrate-based nanoparticles and lectins has not been demonstrated thus far.

Concanavalin A (Con A), a plant lectin, can form a tetramer under an appropriate condition and bind specifically to manno- and glucopyranosides.⁸ Con A is a metalloprotein that requires one Ca^{2+} and one Mn^{2+} per subunit for carbohydrate binding. Physical characterization of Con A revealed mono-dispersity at pH 2-5, suggesting pH-dependent association of subunit, see Figure 4-1.

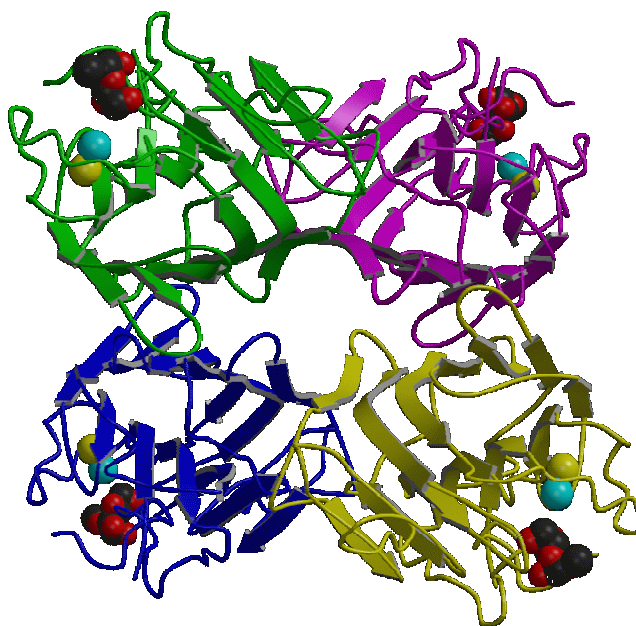


Figure 4-1. The protein structure of Con A.

The binding between Con A and carbohydrates has long been recognized as an excellent system to study the multivalent effects. The multivalent interactions have been studied using various techniques such as electron microscopy,⁹ calorimetry,¹⁰ X-ray crystallography¹¹ and surface plasmon resonance (SPR).¹² These studies have provided information on the Con A and saccharide binding model and interaction

kinetics, which are useful for the development of potent inhibitors and biological effectors.

Previously on Chapter 3, we have demonstrated that mannose-encapsulated gold nanoparticles (*s-6-m-AuNP*) can be used as a probe to target specific protein in living bacteria.¹³ In this chapter, we explore the multivalent interactions between Con A and mannose-, glucose- and galactose-encapsulated gold nanoparticles. The SPR technique is applied to quantitatively analyze the interactions. We found that the binding of *s-6-m-AuNP* to Con A exhibited a strong multivalent effect and that the binding specificity of Con A for the multivalent carbohydrate-encapsulated gold nanoparticles (*carbohydrate-AuNP*) was similar to that of the monovalent counterparts. We also show that the affinity of the *s-6-m-AuNP* to Con A can be adjusted by altering nanoparticle size or sugar moiety. Our results demonstrate that nanoparticles can be excellent multivalent carbohydrate carriers for lectins and that *carbohydrate-AuNP* has a great potential as effective inhibitors of protein-carbohydrate interactions in biological system.

4.2. Result

Various *carbohydrate*-AuNP were synthesized following similar methods as previously chapter (see chapter 2).¹³ The detailed procedures of synthesis and characterization of *carbohydrate*-AuNP are described in supplemental materials. In brief, nearly mono-dispersed gold nanoparticles with averaged diameters of 6 nm or 20 nm were prepared, and their sizes were confirmed using transmission electron microscopy.¹⁴ Various carbohydrate ligands in different linker lengths were synthesized with an S-H group at one side, which was then linked to the nanoparticle through the formation of a strong thiol bond. The amount of carbohydrates attached on each gold nanoparticle was quantitatively determined by the H₂SO₄/phenol assay and elemental analysis.¹⁵

To assess the binding affinity of α -D-methyl-mannopyranoside (α MeMan) and various *carbohydrate*-AuNP for Con A, we utilized the SPR competition binding assay based on the previous report^{12,16} with some modifications. A self-assembled monolayer composed of 20% mannopyranoside ligand and 80% thiobutanol mixture was generated on a J1 biosensor chip (Fig. 4-2).¹⁷

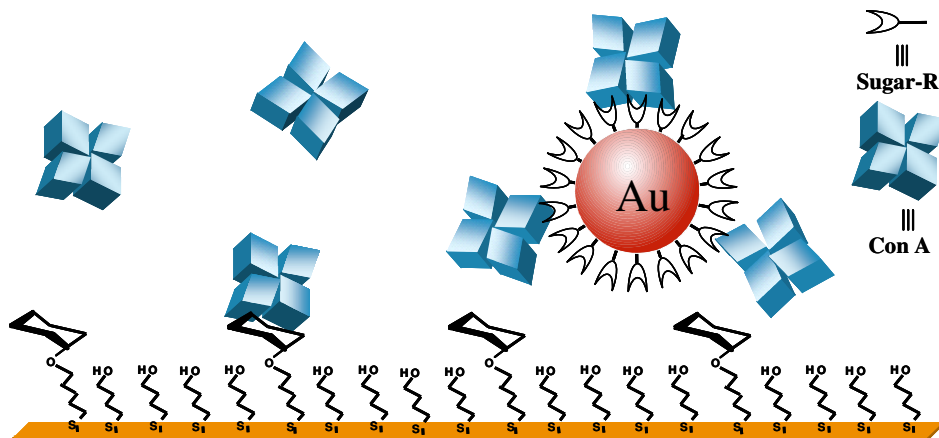


Figure 4-2. BIAcore measurement by J1 Chip of binding affinity between Con A and *carbohydrate*-AuNP.

The affinity of Con A for this chip was determined by titration with series of Con A concentrations to generate multiple SPR response curves. Using the rectangular hyperbolic equation¹⁸ the association constant K_a of Con A for this chip was obtained, and the value was $7.95 \times 10^6 \text{ M}^{-1}$. In competition assays, inhibition curves were generated by measuring the binding responses for $0.5 \mu\text{M}$ Con A tetramer in the presence of different concentrations of αMeMan or *carbohydrate*-AuNP as competitive inhibitors. In Fig. 4-3 to 4-5, we presents a set of SPR response curves for Con A in the presence of mannosepyranoside encapsulated AuNP.

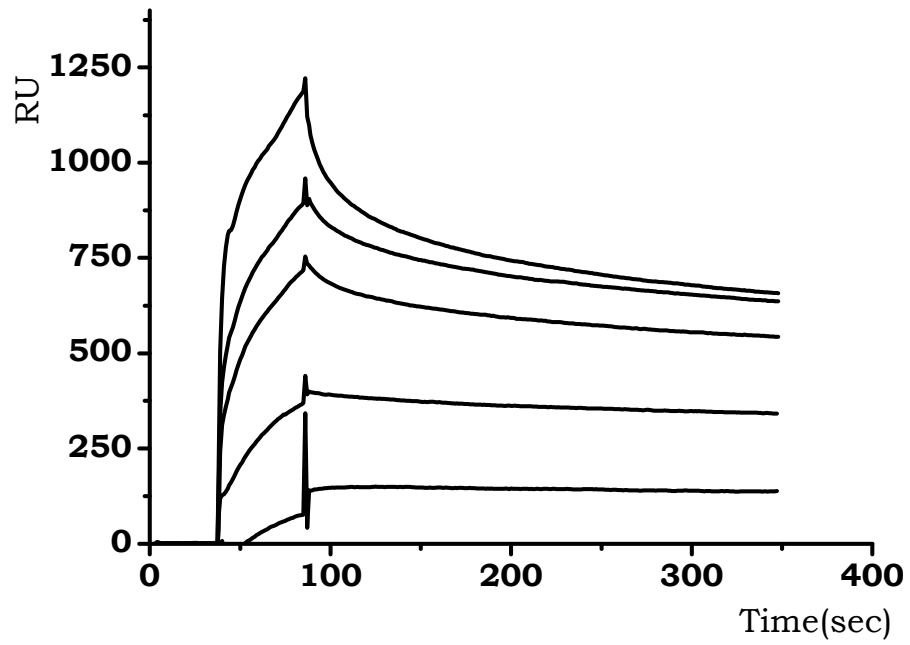


Figure 4-3. A set of curves for 0, 0.875, 1.75, 7, 28 μM αMeMan of Con A (top to bottom) were shown.

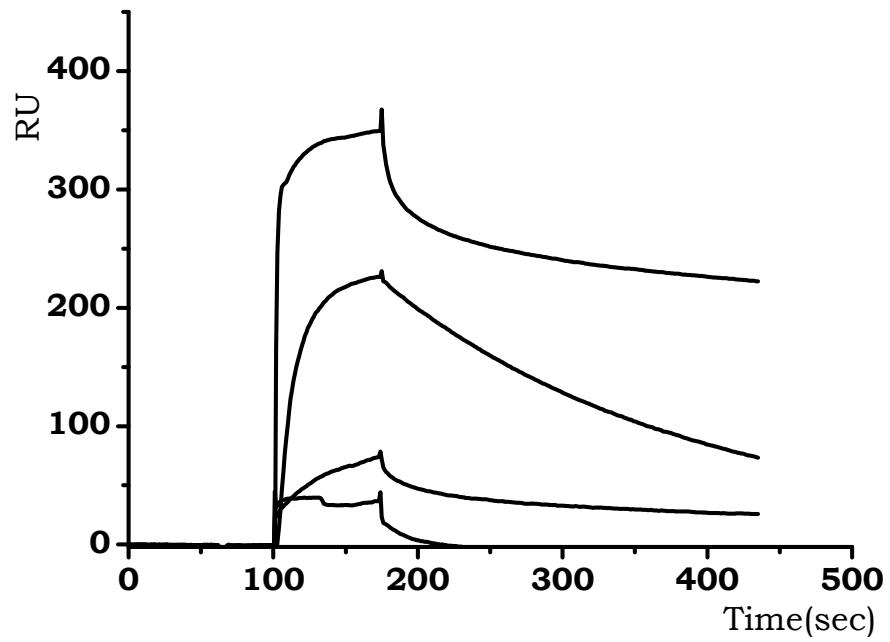


Figure 4-4. A set of curves for 0, 0.175, 0.5, 1 μM *s-6-m-AuNP* of Con A (top to bottom) were shown.

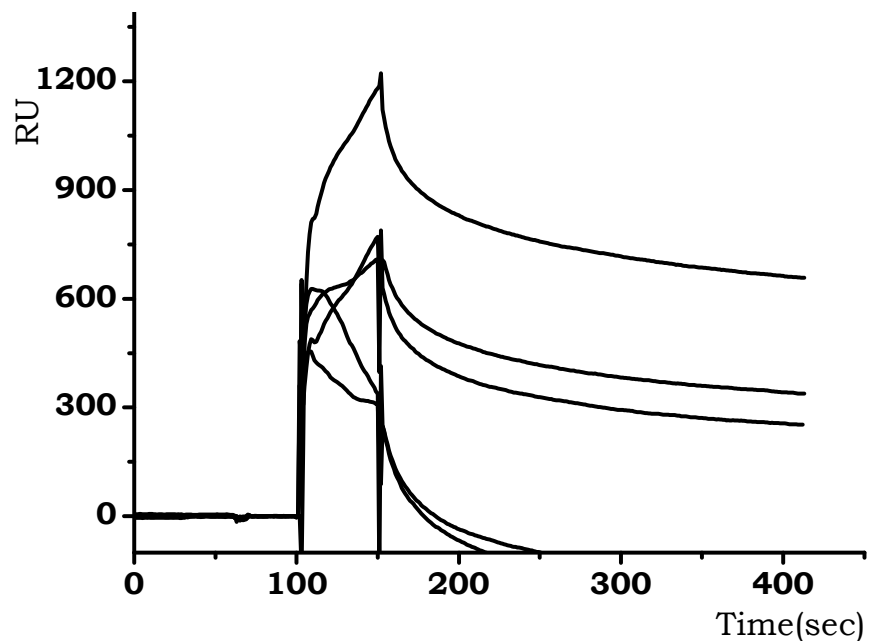


Figure 4-5. A set of curves for 0, 0.175, 0.5, 1 μM *l*-20-*m*-AuNP of Con A (top to bottom) were shown.

From the inhibition curves of each *carbohydrate*-AuNP, its inhibition constant (K_i) is obtained using the equations derived by Attie *et al.*¹⁹ (Table 4). To compare the inhibition potencies of the individual mannose ligand on three different *carbohydrate*-AuNP (*s*-6-*m*-AuNP, *s*- or *l*-20-*m*-AuNP) with respect to monovalent αMeMan , we calculated the relative inhibition potency (RIP).²⁰

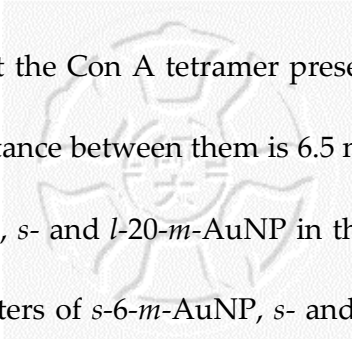
Compound	K_i	RIP
α MeMan	2.0×10^{-4}	1.0
<i>s</i> -6- <i>m</i> -AuNP	8.8×10^{-8}	11.2
<i>s</i> -20- <i>m</i> -AuNP	2.3×10^{-9}	127.8
<i>l</i> -20- <i>m</i> -AuNP	3.5×10^{-9}	67.5
<i>s</i> -6- <i>g</i> -AuNP	1.6×10^{-7}	/
<i>s</i> -6- <i>t</i> -AuNP	—	—

— : no inhibition; / :not determined

Table 4. The data of dissociation constants (K_i) and relative inhibition potency (RIP) of *carbohydrate*-AuNP to Con A.

4.3. Discussion

The RIP values for the mannose ligands of *s*-6-*m*-AuNP, *s*- and *l*-20-*m*-AuNP are from 11 to 128 (Table 4), indicating that the multivalent mannose ligands of *s*-6-*m*-AuNP, *s*- and *l*-20-*m*-AuNP have one to two orders higher affinities to Con A than monovalent mannose ligands. In addition, all *s*-6-*m*-AuNP, *s*- and *l*-20-*m*-AuNP exhibited a stronger inhibition effect than *s*-6-*g*-AuNP and *s*-6-*t*-AuNP. *s*-6-*t*-AuNP displayed no detectable inhibition effect. This is consistent with the previous studies that Con A binds to mannose better than glucose but does not bind to galactose.^{21,12} Therefore, no switch of Con A specificity for carbohydrates clustered on nanoparticles was observed in our system. Taken together, our results demonstrate that clustering of carbohydrate ligands on a nanoparticle significantly enhances the ligand binding affinity for lectins, with no change in lectin binding specificity.



It has been studied that the Con A tetramer presents two saccharide binding sites on each face, and the distance between them is 6.5 nm.²² We compared the inhibition potencies of *s-6-m-AuNP*, *s-* and *l-20-m-AuNP* in the SPR competition assays (Table 1). As the particle diameters of *s-6-m-AuNP*, *s-* and *l-20-m-AuNP* are comparable to or significantly larger than the distance between two relevant binding sites on Con A, respectively, the mannose ligands of *s-6-m-AuNP* are less favorable to engage in the divalent binding of a Con A tetramer than those of *s-20-m-AuNP* and *l-20-m-AuNP*.²³ Our system showed that the carbohydrate ligands with ability to span the requisite distance to occupy two Con A saccharide binding sites are more effective multivalent inhibitors than those fail to engage divalent binding. We further investigated the effects of different linker lengths of *s-* and *l-20-m-AuNP* on Con A binding affinity (Table 4). The two-time difference in the RIP values of *s-* and *l-20-m-AuNP* might be attributed to the differences in their intrinsic properties, for example, the orientation of mannose groups on the surface and/or the rigidity of the linkers.

4.4. Conclusion

We have demonstrated that a nanoparticle can be a good multivalent ligand carrier. The multivalent interactions between *s-6-m-AuNP*, *s-* and *l-20-m-AuNP* and Con A are affected by nanoparticle size and the linker of mannose ligands. Our approaches may be also applicable to other types of nanoparticles such as quantum dots²⁴ and magnetic nanoparticles.